Cerâmica. 2024, v.70:eIEZF8928
ORIGINAL ARTICLE
http://dx.doi.org/10.1590/IEZF8928

Properties and homogeneity of a commercial light expanded clay aggregate

Evelin N. Sosa Fabré[1], Anabella Mocciaro[1]*, Diego Richard[1,2], María S. Conconi[1,2], Nicolás M. Rendtorff[1,2]
[1]CETMIC Centro de Tecnología de Recursos Minerales y Cerámica (CIC-CONICET La Plata-UNLP), Cno. Centenario y 506, 1897, M.B. Gonnet, Argentina.
[2]Facultad de Ciencias Exactas, Universidad Nacional de La Plata, Calle 1 y 47, 1900, La Plata, Argentina.

Abstract

In the present work, an exhaustive analysis of an Argentinian commercial LECA with a multi-technique approach was successfully carried out. Five sub-types of samples were considered to study the degree of macroscopic homogeneity of the LECAs, which presented observable differences in color and morphology. The microstructural, textural, and mineralogical features of the aggregates within each category were assessed and the differences among them were described and discussed. The density values of the samples studied were between 1.01 and 1.20 g/cm^3 and porosity percentages were in the range of 24 to 33 %. The samples present a similar mineralogical composition with quartz and anorthite as the main crystalline phases and almost 50 wt. % of non-crystalline phase. In addition, some variations in the Rietveld quantification were analyzed. The main challenge of LECAs industrial production is to control the raw materials and the process to obtain homogeneous LECAs with similar performance. In this regard, this type of analysis is useful for establishing and comparing some characterization strategies to control, select, design, and evaluate new LECAs.
Keywords: LECA, properties, microstructure, homogeneity

INTRODUCTION

Light expanded clay aggregates (LECA) are ceramics produced from plastic clays [1]. LECAs are inert without harmful materials, with neutral values of pH, they are not damaged by water, non-combustible, and non-biodegradable. In addition, they are good thermal and acoustic insulators and fire resistant [2, 3]. Due to these properties, LECAs are used in a wide range of applications: in the construction field for the production of lightweight blocks, concrete, and precast materials [2, 4, 5, 6, 7]; in filters as sorbents for the removal of polycyclic aromatic hydrocarbons (PAHs) from water [8], in wetlands for treating agricultural wastewaters [9, 10] and as an adsorbent substrate due to its high phosphorus and nitrogen removal capacity in aquaculture wastewater [11].

The aggregates are formed by extrusion or agglomeration with water, then dried and fired. The firing temperature of these materials is in the range of 1050-1250 °C with a dwell time between 3 to 20 min [12, 13, 14]. During firing, the aggregate expands due to two different processes that take place simultaneously [15, 16]:

Gas generation by the thermal decomposition of clays, carbonates, oxides, and the burning of organic material.

Formation of a suitable viscous matrix that produces a pyroclastic state of the material.

Generally, minerals such as clays (illite, montmorillonite), vermiculite, or shale are used as raw materials [17, 18]. The ratio between SiO_2 and Al_2O_3, and fluxing agent content (Na_2O, Fe_2O_3, CaO, K_2O, and MgO) are useful parameters in the design of new materials, to obtain a sufficient degree of viscosity to trap the gas in the pore and achieve the swelling behavior of the aggregate [19, 20].

The parameters that influence the expansion process were defined in literature: mineralogical and chemical composition of the raw materials, size of the clay grains, aggregate size, kiln processes parameters (mass flow, angle, rotation speed, calcination atmosphere, heating rate, temperature and dwell time), and viscosity of the melt [4, 13, 21].

The main challenge of LECAs industrial production is to control the raw materials and the process to obtain homogeneous LECAs with similar performance. In this regard, it is essential to understand which properties most are influenced by variations due to the manufacturing process.

The goal of the present work is to perform an exhaustive analysis of an Argentinian commercial LECA with a multi-technique approach that involves the analysis of the microstructural and textural properties and the mineralogical composition. In addition, to study the degree of macroscopic homogeneity of the LECAs, five categorized sub-types of samples were considered, which presented observable differences in color and shape. The microstructural, textural, and mineralogical features of the aggregates within each category were assessed, and the differences, whether there are, among them were described and discussed. This type of analysis might be useful for the implementation of control, selection, design, and evaluation strategies of new LECAs.

MATERIALS AND METHODS

The commercial LECA aggregates studied in this work

* *amocciaro@cetmic.unlp.edu.ar*
https://orcid.org/0000-0001-7764-067X

were manufactured in Argentina (Superlec, Arcillex S. A.) and are shown in Fig 1. Soil from Buenos Aires province is used as raw material.

Figure 1: Image of the studied LECAs.

The granulometric distribution analysis of a commercial bag (25 kg) was carried out with standard sieves (mesh sizes ¾, ½, ⅜, ¼, and 4), according to the Standard Test Method for Sieve Analysis of Fine and Coarse Aggregates [22] with the addition of the ¼ sieve for aggregates passing the ⅜ sieve.

The whole bag content was observed in a lab table. Some variations in color and morphology were found with the naked eye. This was the reason for dividing the content into five categories and characterizing them. Ten aggregates of each category were studied using the Munsell soil color chart [23]. The macroscopic morphology (sphericity and roundness) was classified using a visual comparison chart [24].

The five categories of LECAs were studied by a multi-technique ceramic approach. Apparent density, open porosity, and water absorption were evaluated by the Archimedes immersion method in water according to ASTM C 83 [25]. Open pore size distribution was analyzed by a mercury intrusion porosimeter (Thermo Scientific Pascal 440 Series equipment) [26]. A stereoscopic microscope (Leica SAPO) and a scanning electron microscope (SEM) were used to analyze the microstructure. SEM micrographs were taken on silver-coated polished surfaces (1.0 μm diamond paste) in ultrahigh vacuum conditions (JEOL equipment JCM-6000 model).

The crystalline phases of the aggregates were determined by powder X-ray diffraction (XRD), using CuKα radiation operating at 40 kV and 30 mA (Bruker D8 Advance A25). For this purpose, samples were ground to a fine powder. Also, powders from the aggregate core and external surface were considered. The XRD patterns in the 3–70° range were analyzed with the program FullProf [27], which is a multipurpose pro-file-fitting program, including Rietveld refinement to perform phase quantification [28] and Le Bail approach to quantify glassy/amorphous phases [29].

Finally, the LECA thermal stability was evaluated by thermogravimetric and differential thermal analysis (DTA-TG) simultaneously (Rigaku Evo II equipment) with 10 °C min^{-1} as the heating rate and a temperature range of 25-1000 °C. To this purpose, (29.13±0.01) mg of the sample was placed in a Pt crucible in an air atmosphere, and alumina was used as a reference.

RESULTS AND DISCUSSION

Size, color, and morphology of the studied LECAs

The granulometric distribution showed that all the samples passed the ¾ mesh, 42 wt. % was retained in ½ mesh, 49 wt. % was retained in ⅜ mesh and 9 wt. % was retained in ¼ mesh. This test determined that the largest number of aggregates have a size between 9-19 mm. The standard ISO 20290 [30] defined that aggregates from 0 to 3 mm are used for blocks, small pre-casted pieces, concrete, mortars, and asphalt concrete; aggregates from 3 to 10 mm for structural

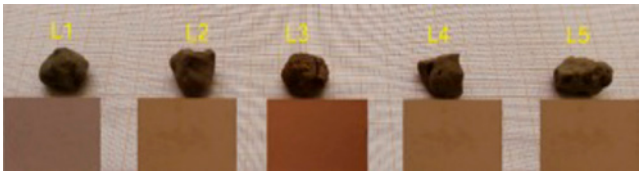

Figure 2: Representative image of the five identified groups and their respective color.

Table I. Mass percentage, Munsell color (Hue, Value, and Chroma), and morphologic parameters for the five categories of LECAs.

Sample	wt. %	Hue	Value	Chroma	Roundness	Sphericity
L1	48	7.5YR	6	2	Very angular and sub-angular	Sub-discoidal
L2	21	5YR	6	4	Rounded	Sub-prismatic
L3	20	2.5YR	6	4	Sub-rounded	Sub-discoidal
L4	7	5YR	6	4	Rounded	Sub-prismatic, sub-discoidal, and spherical
L5	4	5YR	6	4	Sub-angular	Sub-discoidal

Table II. Density, open porosity, water absorption, and pore diameter of samples L1-L5 (standard deviation in brackets).

Sample	Apparent density (g/cm^3)	Open porosity (%)	Water absorption (%)	d10 (nm)	d90 (nm)
L1	1.03 (0.04)	32 (3)	32 (2)	50	3200
L2	1.03 (0.04)	30 (3)	31 (2)	50	2500
L3	1.20 (0.02)	24 (3)	21 (2)	75	3300
L4	1.03 (0.09)	29 (5)	21 (1)	120	3600
L5	1.01 (0.05)	33 (4)	35 (2)	80	4200

concrete, pre-stressed concrete, asphalt concrete, subfloors, and refractory castables and those from 10 to 20 mm for insulating subfloors, drainage, and refractory concrete. Considering this classification the studied LECAs can be used in the last category.

The five categories according to color and morphology were labeled L1, L2, L3, L4, and L5. In Fig. 2 a representative aggregate for each group is shown. The mass percentage, color, and morphologic parameters of each category are presented in Table I. The L1 sample represents almost half of the mass of the whole batch, meanwhile, L4 and L5 have the lowest mass percentages.

Munsell parameters are: hue, which represents the color of the sample; value, which indicates how light or dark a color is and chroma which represents the intensity of the color. The studied aggregates present a homogenization of its lightness with a number 6 that represents the middle within dark and light.

All the samples are identified as yellow-red with some differences in the ratio yellow/red; L2, L4, and L5 have the highest relation (7.5 parts yellow and one part red meanwhile L3 has the lowest ratio (2.5 parts of yellow and one part of red). The chroma presents homogeneity from L2 to L5 with a medium number (the maximum value for the chroma parameter is 8), while L1 presents the lowest number.

The differences observed using this method represent the differences observed with the naked eye when analyzing the batch of commercial LECAs studied. Based on these results, a systematic analysis could be implemented using the Munsell scale.

As in all granular ceramic materials, the morphological characteristics influence the structural behavior and strength of the aggregates [31]. In general, the aggregates present low sphericity and roundness. The sphericity is equal for samples L1, L3, and L5, presenting a qualification of sub-discoidal. On the other hand, L2 is identified as sub-prismatic, and L4 is a mix of sub-discoidal, spherical, and sub-prismatic. Regarding roundness, L1 is identified as sub-angular and very angular, L2 and L4 as rounded, L3 as sub-rounded, and L5 as sub-angular. Aggregate shape is directly related to the expansion during firing and is an important parameter for some applications, low sphericity and roundness could reduce packing density in concrete [20, 32].

Texture properties

In Table II the values of apparent density, open porosity, water absorption, and pore size percentiles are presented. The values of density are between 1.01 and 1.20 g/cm^3, porosity is in the range of 24-33 %, and water absorption is between 21 and 35 %. Samples L1, L2, L4, and L5 present similar values of apparent density. On the other hand, L3 has a greater density (20 % higher) and the lowest open porosity, showing that this subtype of LECA presents a different sintering grade. According to the literature, LECAs can be classified into four groups based on their density: very low density (0.3-0.6 g/cm^3), low density (0.61-0.99 g/cm^3), medium density (1.0-1.4 g/cm^3), and high density (>1.4 g/cm^3) [15]. Considering this classification the studied aggregates have values of medium density and could be used in concrete for building construction [1]. In addition, water absorption must be considered when analyzing the application of the aggregates; if LECAs are to be used in the manufacture of concrete, water absorption must be considered in the calculation of the amount of water required in the mix [33].

The pore size distribution of the studied aggregates is shown in Fig. 3 and the derivative curves are plotted in the inset. In general, the pore distribution is in the range of 50-

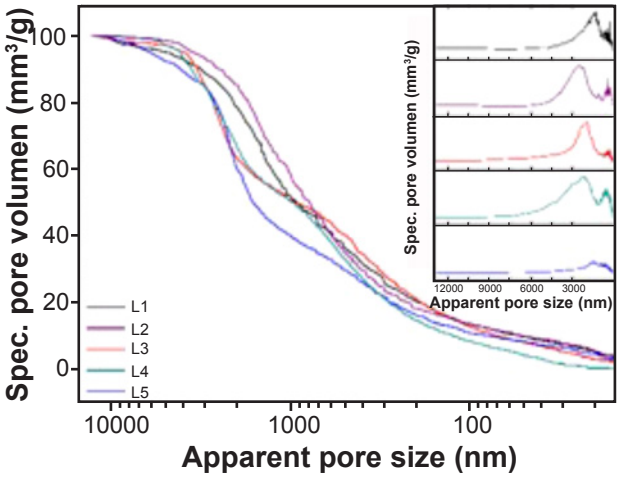

Figure 3: Open pore size distribution of the five LECAs studied by Mercury Intrusion Porosimetry.

4500 nm. To describe each distribution span, particle size at 10% and 90% of the cumulative size distribution are included in Table II (diameters d10 and d90, respectively). The distributions in Fig. 3 are similar between L1 and L2 samples, as well as between L3 and L4. Instead, the pore size distribution in L5 differs from that of the other samples. On the other hand, the derivative curves show a bimodal distribution with pores in two ranges, one between 200-800 nm and the other between 1000-9000 nm. The first one was not observed in the L5 sample.

Microstructure

Fig. 4 shows stereo microscope images of a representative aggregate of each category. The samples present a red external surface and a black core with some white inclusions. The red external surface has a thickness between 0.16 and 0.26 mm and is related to oxidative processes during heat treatment. Some cracks are observed in the external surface, which sometimes extend to the black core, generating a red area on the inside of the aggregate. The black core is produced during the heat treatment by a reducing atmosphere [1]. Therefore, from the microscope inspection can be concluded that oxidation and reduction processes acted simultaneously in each aggregate. The observed white inclusions have a size of 0.08 to 0.7 mm and are effervescent in contact with hydrochloric acid. This allowed determining that they are carbonates.

Inside each aggregate, a vesicular structure with pores of different sizes from 0.04 to 3 mm is observed. The shape of the pores is varied, some are rounded, others channel-shaped, and others elongated. The pores often end in cracks up to 3 mm in length. The cracks could evidence a fast cooling; during this process, the core and the external surface can be at different thermal shrinkage which might induce the formation of micro-cracks that reduce the aggregate strength [34].

SEM images of L1 to L5 were taken to analyze with more detail the microstructure. Representative results are presented in Fig. 5. Images labeled with the letter A correspond to the external surface and images labeled with the letter B correspond to the core of the LECA. In general, all the samples present a rough external surface with microcrystals and a core with pores embedded in a vitreous matrix. According to the literature, the amount of the vitreous phase is responsible for allowing or not the visualization of the crystals [35]. This contrast between aggregate external surface and core microstructure was also observed in other works [36, 37, 38].

In Fig. 5, different morphologies for the pores in the amorphous glassy phase can be distinguished: spherical pores, channels, and pore junctions are observed. Also, some minor pores are detected in the walls. Crystals are occluded within pores, and partitions typical of the vesicular texture, with or without porosity, are observed. Pore sizes range between 0.2 and 70 µm and crystal sizes between 0.3 and 5 µm were observed. Very large pores were identified, for example in image L5B, that could be associated with excessive swelling caused by the simultaneous gas release and low pyroplastic viscosity [39].

The bloating process can be divided into two effects: macro-bloating, which is related to the macroscopic expansion of the aggregate that grows in volume from 3 to 5 times; and micro-bloating, which corresponds to the pores

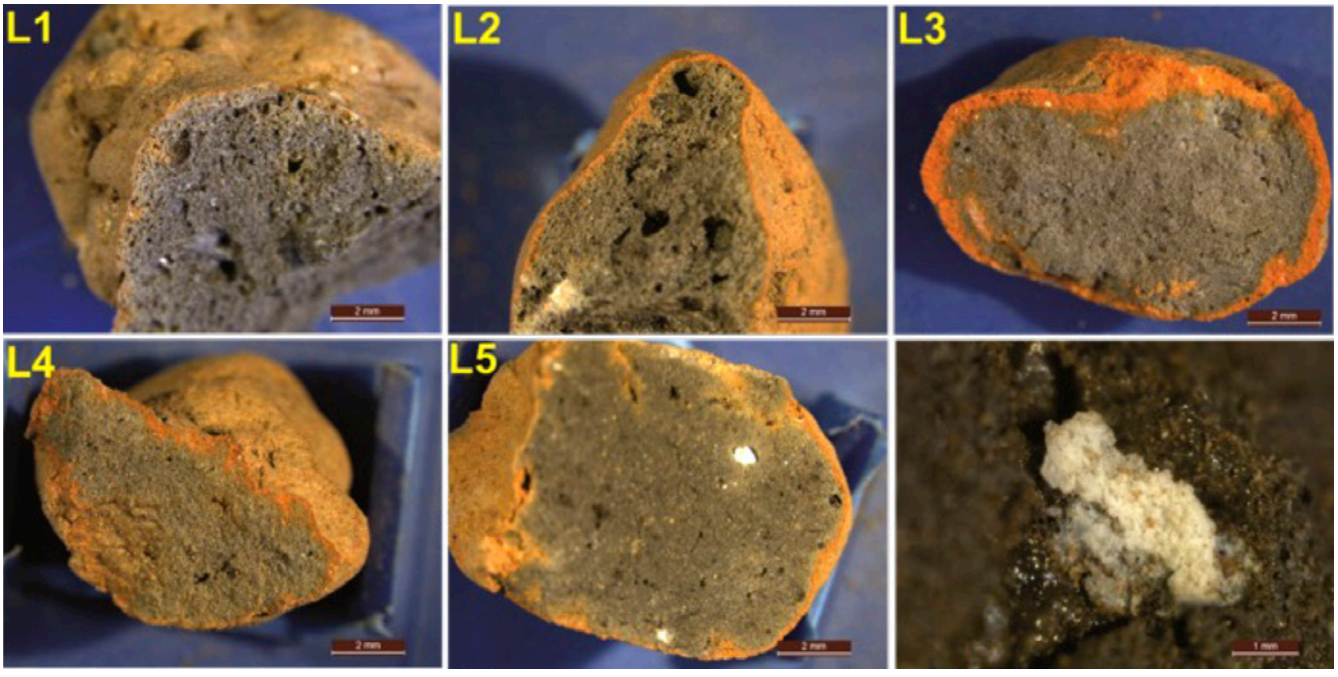

Figure 4: Cross-section images of the interior and external surface of the studied LECAs (L1-L5). A detail of a carbonate inclusion is in the low-right image.

developed in the internal vesicular texture. This vesicular structure is observed in the samples by SEM and could be evidence of the bloating process [15, 40].

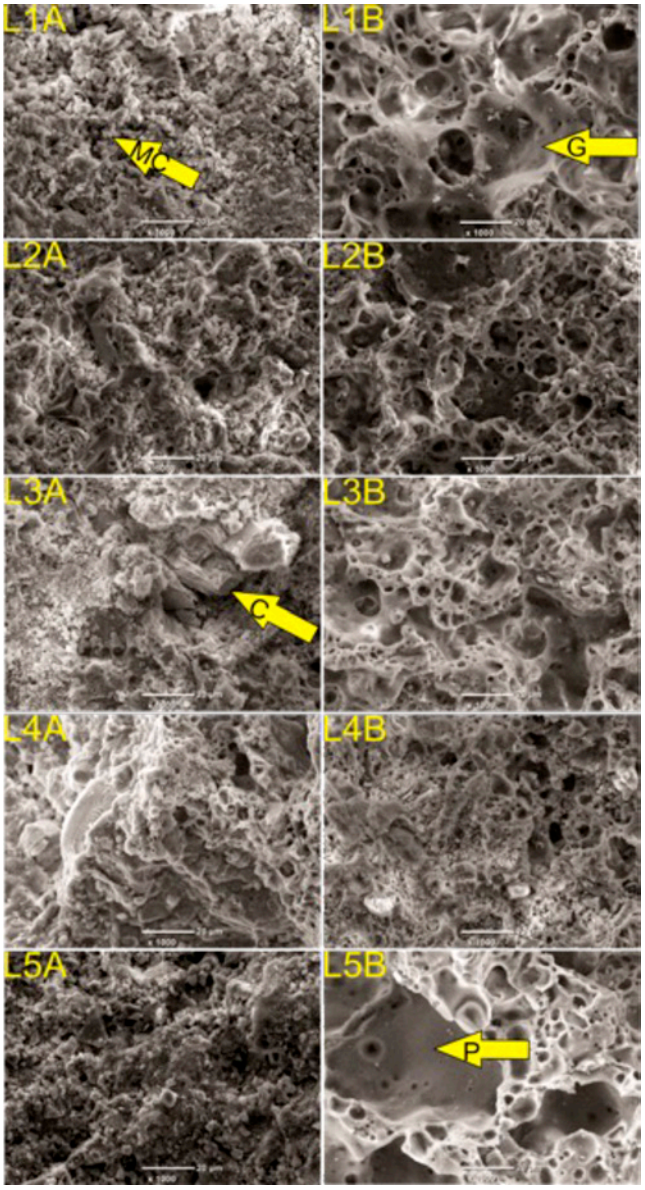

Figure 5: SEM images. A: external surface, B: core. Magnification x1000. (The labels correspond to examples of pores (P), glassy phases (G), microcrystals (MC), and larger crystals (C)).

In the studied LECAs, the initial morphology of the aggregates before the firing process is not known but, based on the sphericity parameters shown in Table I and the microstructure analysis, the macro and micro bloating process effects can be observed. Based on the microstructural analysis, the studied LECAs can be interpreted as materials with a relevant degree of heterogeneity, this might be explained by heterogeneities in the formulation and imperfections in the forming process. The presence of inclusions can be attributed to insufficient disaggregation, grinding, and/or sieving, as well as using raw materials with a varied grain size. On the other hand, cracks could be attributed to poor compaction during forming and/or a poorly controlled drying process. In addition, cracks also could appear due to the sintering process that is carried out at higher heating rates than other traditional and industrial ceramic materials. The microstructure analysis performed by stereo microscope and SEM also allowed observing pores with higher sizes than those measured by mercury intrusion porosimetry.

Crystalline phases of the studied LECA.

Fig. 6 shows X-ray diffraction patterns of the studied LECAs. The crystalline and non-crystalline phases of the studied LECAs were analyzed by XRD, and the neoformed phases were identified. These are strongly related to the material physical and technological properties [1]. The main crystalline phases are quartz and anorthite, with a small amount of hercynite meanwhile microcline is only identified in the L3. Crystalline phases identified in the studied LECA (see Fig. 6) are like those reported in the literature and correspond to the common raw materials frequently used for the manufacture of LECA [41,42, 43]. Because the raw materials used in the fabrication of LECAs are clays composed of quartz, feldspars, and calcite, it is common to find quartz and anorthite in the LECAs, because the fired temperature is 1100-1300 °C. Furthermore, some traces of hematite are identified in all the samples. Table III summarizes the chemical formula of the crystalline phases identified by XRD and the Powder Diffraction Files (PDF) cards used as references.

Fig. 7 presents Rietveld quantification results for the crystalline phase, the Le Bail approximation for the non-

Table III. Identified crystalline phases, and chemical formula, and employed PDF card.

Crystalline phase	Chemical formula	PDF card
Quartz	SiO_2	00-046-1045
Plagioclase	$(Ca, Na)(Si, Al)_4O_8$	00-018-1202
Hercynite	$FeAl_2O_4$	01-085-1828
Microcline	$KAlSi_3O_8$	00-019-0932
Glassy phase	Silica (SiO_2) based	Le Bail approach

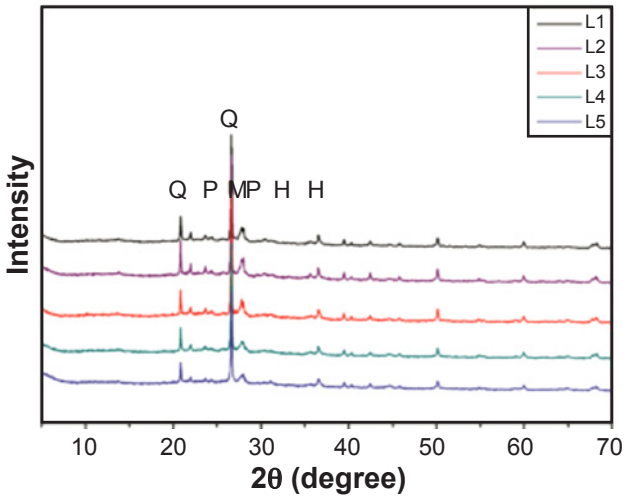

Figure 6: XRD patterns of the studied LECAs (Q: quartz, P: plagioclase; M: microcline, H: hercynite).

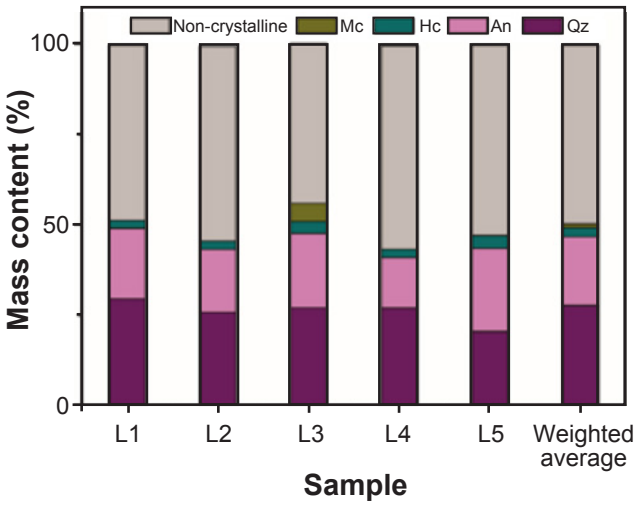

Figure 7. Rietveld crystalline phase quantification results (Mc: microcline; Hc: hercynite; An: plagioclase; Qz: quartz).

crystalline phase, and the weighted average of all the samples. The weighted profile *R*-factor (*Rwp)* values are between 24.4 to 26.8, these indicate the goodness of the refinements and are like that reported in the literature for this type of ceramic material [44]. Non-crystalline phase is around 50 wt.% in all the samples, the greatest percentage of the non-crystalline phase is identified in sample L4 (56.3 wt. %) and the lowest one is identified in L3 (44.2 wt. %). The amount, viscosity, and chemical composition of the non-crystalline phase are related to the expansion process in the thermal treatment [9]. Quartz percentage is greater in all the samples than anorthite percentage, except in the L5 sample where this relation is inverted. In all the samples hercynite content is lower than 3.5 wt. %. The presence of quartz and anorthite is useful in the drying process of any ceramic since they limit the shrinkage during the drying process and avoid the cracking development of the material [45].

Considering the mass percentage of each category determined above (section 3.1), the sample L1 mineralogical composition should be considered the most representative of the studied LECAs. This is also reflected in Fig. 7 through the similarity between sample L1 and weighted average results.

Regarding the identification of the crystalline phases in the black core, they are the same as those identified in the powder obtained from the whole sample (Fig. 8). Meanwhile hematite (Fe_2O_3) is identified as one of the crystalline phases in the aggregate external surface. This difference between the external surface and the core suggests that the thermal treatment was performed in an atmosphere with a low content of oxygen. On the other hand, using a magnet over the black core powder it was detected a magnetic behavior that is assigned to magnetite. The presence of magnetite and hercynite indicates that the thermal treatment during the LECAs manufacture was in a reducing atmosphere with temperatures higher than 1050 °C [41, 46].

Crystalline phases identified in all the samples are the same. This homogeneity is reflected in the similar values obtained in the technological properties. The differences

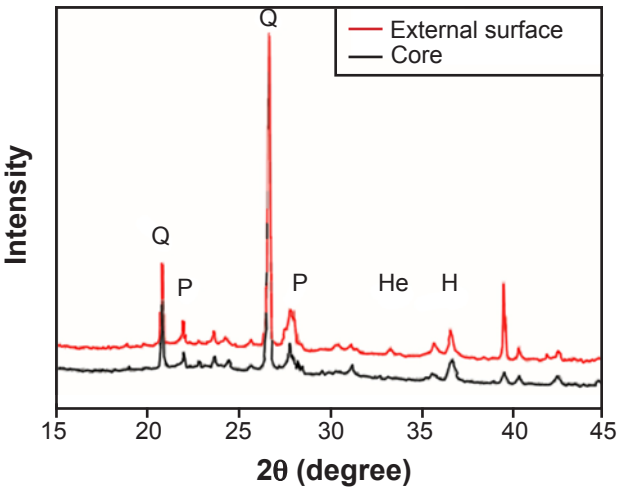

Figure 8. XRD patterns of the aggregate external surface and black core (Q: quartz, P: plagioclase; H: hercynite; He: hematite).

observed in the Rietveld quantification could be explained by two reasons. Firstly, is related to the variation of the heat treatment in the rotary kiln, some aggregates could stay longer in the hot zone or be in a shorter cycle depending on the mass flow. Rotary kilns have a good performance, but it is well known that it is possible for the materials to undergo different thermal cycles and, therefore, different physical-chemical processes can occur in them.

Secondly, it could be since the raw material used is natural clay, it is not possible to have a homogeneous composition, resulting in variations in the presence of carbonate inclusions, as was already mentioned in section 2.3. In addition, in the process of mixing and grinding raw materials on an industrial scale, variations in the composition of each aggregate can be generated.

Thermal behavior and stability of the studied LECA

DTA–TG analyses were carried out to know the thermal

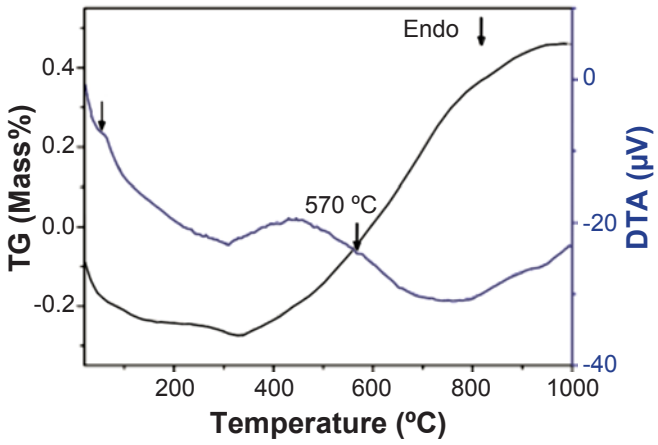

Figure 9. Thermogravimetric (TG) and Differential thermal analysis (DTA) of the studied LECA.

stability of the aggregates. Fig. 9 shows the DTA-TG curves of sample L3 as representative of all the samples studied in this work. In the TG curve a mass loss of 0.24 wt. % between room temperature and 140 °C is observed, which is also accompanied by the endothermic peak at 62 °C in the DTA curve that is related to the free and adsorbed water loss from the LECA.

Afterward, a mass gain of 0.7 wt. % is observed in the TG curve between temperatures 300-1000 °C. This might be explained by the oxidation by the presence of Fe (II) species. For example, this mass gain would correspond to approximately 5% of oxidation of Fe (II) oxide during the heating process. However, this thermal process would be overlapped by the possible mass loss resulting from the combustion of the un-combusted carbon below 800 ºC, possibly present in the aggregate core. On the other hand, an endothermic peak at 570 °C is observed in the DTA curve, which is related to the α→β phase transformation of quartz [47, 48].

CONCLUSIONS

In this work, a comprehensive characterization of an Argentinian commercial LECA was carried out from a ceramic point of view including microstructural, textural, and mineralogical analyses. Considering the variation in homogeneity observed in a simple visual analysis of a commercial bag of this LECA, five categories were proposed. Representative samples of each category were studied and compared.

The results of this multi-technique characterization allowed a deep description of the LECAs as ceramic aggregates with low roundness and sphericity. The textural properties indicate that these LECAs can be classified as medium apparent density aggregates (1.0-1.2 g/cm^3). The LECAs presented a clear vesicular-type microstructure, with pores and channels corresponding to the slight bloating mechanism (micro-bloating). Some cracks were observed that could be evidence of a fast cooling process. No important differences between the five categories were observed in their microstructure or their bloating process.

Non-crystalline phase presents around 50 wt.% in all the samples and between crystalline phases the majority are quartz and anorthite. Also, the five categories present an oxidized external surface and an unoxidized black core with evidence of magnetic behavior assigned to magnetite. According to the crystalline phases identified in the samples, the thermal treatment of the aggregates was above 1050 °C and the firing atmosphere was mild reductive, with a low surface oxygen penetration (less than 1 mm).

The main differences between the five categories were observed in density and mineralogical composition, particularly in the L3 sample. This sample presents the major apparent density and microcline in its mineralogical composition. This could be for the thermal treatment and the differences in the dwell on the hot zone of the rotary kiln and also could be for the nonhomogeneity in the raw material composition.

Among the differences found between the five categories studied, the technological properties of these aggregates fulfill the industrial requirements.

The proposed analysis criteria based on color and morphology proved to be effective in showing small differences or variations in the properties of the materials to obtain homogeneous LECAs with similar performance. Therefore, the present work provides insights that help to establish new characterization strategies for the design, control, selection, and evaluation of LECAs.

ACKNOWLEDGEMENTS

This work was partially supported by ANPCyT (PICT-2021-00225 and PICT-2021-00392), CONICET (PIP 2021-00352), and Facultad de Ciencias Exactas, Universidad Nacional de La Plata (2015–2018 X-737). ENSF thanks CONICET for the fellowship, AM, DR, and NMR are members of CONICET.

REFERENCES

[1] Ayati B, Ferrándiz-Mas V, Newport D, Cheeseman C. Use of clay in the manufacture of lightweight aggregate. Constr. Build. Mater. 2018;**162**:124. doi:10.1016/j.conbuildmat.2017.12.018.

[2] Youssf O, Hassanli R, Mills JE, Abd Elrahman M. An experimental investigation of the mechanical performance and structural application of LECA-Rubcrete. Constr. Build. Mater. 2018;**175**:239. doi:10.1016/j.conbuildmat.2018.04.184.

[3] Rodrigues HKS, Oliveira HAD, Melo FMC, Almeida VGO. Perfil epidemiológico dos casos com microcefalia atendidos em maternidade de alto risco em Sergipe. Rev. Matér. 2022;27. doi:10.17267/2317-3378rec.v10i1.3558.

[4] González-Corrochano B, Alonso-Azcárate J, Rodas M, Barrenechea JF, Luque FJ. Microstructure and mineralogy of lightweight aggregates manufactured from mining and

industrial wastes. Constr. Build. Mater. 2011;**25**:3591. doi:10.1016/j.conbuildmat.2011.03.053.
[5] Ozguven A, Gunduz L. Examination of effective parameters for the production of expanded clay aggregate. Cem. Conc. Compo. 2012;**34**:781. doi:10.1016/j.cemconcomp.2012.02.007.
[6] Bicer A. Retraction notice to "Behaviour of RC flat slabs with openings strengthened with CFRP" [Case Stud. Constr. Mater. 15 (2021) e00587]. Case Stud. Constr. Mater. 2021;15. doi:10.1016/j.cscm.2022.e01220.
[7] Rodrigues AV, Bragança SR. Technological properties of a self-bloating clay and expanded-clay aggregate for the production of lightweight concrete. Cerâmica. 2023;**69**:6. doi:10.1590/0366-69132023693893308.
[8] Nkansah MA, Christy AA, Barth T, Francis GW. The use of lightweight expanded clay aggregate (LECA) as sorbent for PAHs removal from water. J. Hazard. Mater. 2012;**217–218**:360. doi:10.1016/j.jhazmat.2012.03.038.
[9] Dordio A, Carvalho AJP. Constructed wetlands with light expanded clay aggregates for agricultural wastewater treatment. Sci. Total Environ. 2013;**463–464**:454. doi:10.1016/j.scitotenv.2013.06.052.
[10] Mlih R, Bydalek F, Klumpp E, Yaghi N, Bol R, Wenk J. Light-expanded clay aggregate (LECA) as a substrate in constructed wetlands – A review. Ecol. Eng. 2020;**148**:105783. doi:10.1016/j.ecoleng.2020.105783.
[11] Hamid SHA, Lananan F, Noor NAM, Endut A. Physical filtration of nutrients utilizing gravel-based and lightweight expanded clay aggregate (LECA) as growing media in aquaponic recirculation system (ARS). Aquac. Eng. 2022;**98**:102261. doi:10.1016/j.aquaeng.2022.102261.
[12] Rashad AM. Lightweight expanded clay aggregate as a building material – An overview. Constr. Build. Mater. 2018;**170**:757. doi:10.1016/j.conbuildmat.2018.03.009.
[13] Bayoussef A, Loutou M, Taha Y, Mansori M, Benzaazoua M, Manoun B, Hakkou R. Use of clays by-products from phosphate mines for the manufacture of sustainable lightweight aggregates. J. Clean. Prod. 2021;**280**:124361. doi:10.1016/j.jclepro.2020.124361.
[14] Ren P, Ling TC, Mo KH. Recent advances in artificial aggregate production. J. Clean. Prod. 2021;**291**:125215. doi:10.1016/j.jclepro.2020.125215.
[15] Dondi M, Cappelletti P, D'Amore M, de Gennaro R, Graziano SF, Langella A, Raimondo M, Zanelli C. Lightweight aggregates from waste materials: Reappraisal of expansion behavior and prediction schemes for bloating. Constr. Build. Mater. 2016;**127**:394. doi:10.1016/j.conbuildmat.2016.09.111.
[16] Arioz O, Kilinç K, Kaya G, Arslan G, Tuncan M, Tuncan A, Korkut M, Kivrak S. Statistical distributions of in situ microcore concrete strength. J. Aust. Ceram. Soc. 2008;**44**:23. doi:10.1016/j.conbuildmat.2011.06.038.
[17] Mahmad Nor A, Yahya Z, Abdullah MMA, Abdul Razak R, Jaya Ekaputri JJ, Faris MA, Nur Hamzah H. A Review on the Manufacturing of Lightweight Aggregates Using Industrial By-Product. MATEC Web Conf. 2016;**78**:01067. doi:10.1051/matecconf/20167801067.
[18] Moreno-Maroto JM, Cobo-Ceacero CJ, Uceda-Rodríguez M, Cotes-Palomino T, Martínez García C, Alonso-Azcárate J. Mineralogical Evolution of Artificial Aggregates Manufactured with Different Iron Phases. Constr. Build. Mater. 2020;**247**:118583. doi:10.2139/ssrn.4736212.
[19] Wie YM, Lee KG. Composition design of the optimum bloating activation condition for artificial lightweight aggregate using coal ash. J. Korean Ceram. Soc. 2020;**57**:220. doi:10.1007/s43207-020-00025-0.
[20] Lee KH, Lee KG, Lee YS, Wie YM. Manufacturing and application of artificial lightweight aggregate from water treatment sludge. J. Clean. Prod. 2021;**307**:127260. doi:10.1016/j.jclepro.2021.127260.
[21] Molinari C, Zanelli C, Guarini G, Dondi M. Bloating mechanism in lightweight aggregates: Effect of processing variables and properties of the vitreous phase. Constr. Build. Mater. 2020;**261**:119980. doi:10.1016/j.conbuildmat.2020.119980.
[22] ASTM. Test Method for Sieve Analysis of Fine and Coarse Aggregates. ASTM C 136-06 Standard Test Method for Sieve Analysis of Fine and Coarse Aggregates. 2015. doi:10.1520/c0136.
[23] Ruck L, Brown CT. Corrigendum to "Obsidian in the Tavoliere, Southeastern Italy — A regional study". J. Archaeol. Sci. Rep. 2018;**20**:284–292. doi:10.1016/j.jasrep.2018.09.013.
[24] Powers MC. A New Roundness Scale for Sedimentary Particles. SEPM J. Sediment. Res. 1953;**23**:117. doi:10.1306/d4269567-2b26-11d7-8648000102c1865d.
[25] ASTM. Test Methods for Apparent Porosity, Liquid Absorption, Apparent Specific Gravity, and Bulk Density of Refractory Shapes by Vacuum Pressure. ASTM C 83-00. 2011. doi:10.1520/c0830-00.
[26] Chung HSY, Sikora P, Kim DJ, El Madawy ME, Abd Elrahman M. Effect of different expanded aggregates on durability-related characteristics of lightweight aggregate concrete. Mater. Charact. 2021;**173**:110907. doi:10.1016/j.matchar.2021.110907.
[27] Ward C, French D. Determination of glass content and estimation of glass composition in fly ash using quantitative X-ray diffractometry. Fuel. 2006;**85**:2268. doi:10.1016/j.fuel.2005.12.026.
[28] Rietveld HM. A profile refinement method for nuclear and magnetic structures. J Appl Crystallogr. 1969;**2**:65. doi:10.1107/s0021889869006558.
[29] Le Bail A. Modelling the silica glass structure by the Rietveld method. J. Non-Cryst. Solids. 1995;**183**:39. doi:10.1016/0022-3093(94)00664-4.
[30] ISO. European (EN) and World (ISO) Standards—Comparison with ASTM Standards. ISO 20290 Aggregates for concrete. 2021. doi:10.1520/cca10601j.
[31] Nunes JJBDC, Teixeira AMAJ, Saraiva RMDC. Caracterização morfológica do agregado leve de argila expandida brasileira com utilização do AIMS. Ambient. Constr. 2021;**21**:213. doi:10.1590/s1678-86212021000300547.

[32] Souza NSL, Anjos MAS, Sá MVA, Farias EC, Souza MM, Branco FG, Pereira A. Evaluation of sugarcane bagasse ash for lightweight aggregates production. Constr. Build. Mater. 2021;**271**:121604. doi:10.1016/j.conbuildmat.2020.121604.
[33] Alqahtani FK, Zafar I. Characterization of processed lightweight aggregate and its effect on physical properties of concrete. Constr. Build. Mater. 2020;**230**:116992. doi:10.1016/j.conbuildmat.2019.116992.
[34] Bernhardt M, Tellesbø H, Justnes H, Wiik K. The effect of heat treatment and cooling rate on the properties of lightweight aggregates. J. Eur. Ceram. Soc. 2014;**34**:1353. doi:10.1016/j.jeurceramsoc.2013.11.005.
[35] Moreno-Maroto JM, González-Corrochano B, Alonso-Azcárate J, Rodríguez L, Acosta A. Assessment of crystalline phase changes and glass formation by Rietveld-XRD method on ceramic lightweight aggregates sintered from mineral and polymeric wastes. Ceram. Int. 2018;**44**:11840. doi:10.1016/j.ceramint.2018.03.274.
[36] Roces-Alonso E, Estaire J, Martín-Ruiz M, González-Galindo J. Experimental study on lightweight expanded clay at particle level: Breakage of isolated grains. J. Rock Mech. Geotech. Eng. 2023;**15**:1846. doi:10.1016/j.jrmge.2022.12.022.
[37] Movahedi N, Linul E. Mechanical properties of Light Expanded Clay Aggregated (LECA) filled tubes. Mater. Lett. 2018;**217**:194. doi:10.1016/j.matlet.2018.01.078.
[38] Bogas JA, Mauricio A, Pereira MFC. Microstructural Analysis of Iberian Expanded Clay Aggregates. Microsc. Microanal. 2012;**18**:1190. doi:10.1017/s1431927612000487.
[39] Ayati B, Molineux C, Newport D, Cheeseman C. Manufacture and performance of lightweight aggregate from waste drill cuttings. J. Clean. Prod. 2019;**208**:252. doi:10.1016/j.jclepro.2018.10.134.
[40] Wie Y, Lee K. Optimum Bloating-Activation Zone of Artificial Lightweight Aggregate by Dynamic Parameters. Materials. 2019;**12**:267. doi:10.3390/ma12020267.
[41] Santos FF, Santos FLDA, Santos JNS, Pereira MHN, Almeida VG, Melo FMCD, Oliveira HAD, Risso SSO. Estudo da variação granulométrica de agregado sintético para Fabricação de placas pré-moldadas de concreto não estrutural. Rev. Matér. 2018;**23**:11971. doi:10.1590/s1517-707620170001.0307.
[42] Roces E, Muñiz-Menéndez M, González-Galindo J, Estaire J. Lightweight expanded clay aggregate properties based on laboratory testing. Constr. Build. Mater. 2021;**313**:125486. doi:10.1016/j.conbuildmat.2021.125486.
[43] Dordio AV, Teimão J, Ramalho I, Carvalho AJP, Candeias AJE. Selection of a support matrix for the removal of some phenoxyacetic compounds in constructed wetlands systems. Sci. Total Environ. 2007;**380**:237. doi:10.1016/j.scitotenv.2007.02.015.
[44] Conconi MS, Morosi M, Maggi J, Zalba PE, Cravero F, Rendtorff NM. Thermal behavior (TG-DTA-TMA), sintering and properties of a kaolinitic clay from Buenos Aires Province, Argentina. Cerâmica. 2019;**65**:227. doi:10.1590/0366-69132019653742621.
[45] Dondi M. Feldspathic fluxes for ceramics: Sources, production trends and technological value. Resour. Conserv. Recyc. 2018;**133**:191. doi:10.1016/j.resconrec.2018.02.027.
[46] Gliozzo E. Ceramics investigation: research questions and sampling criteria. Archaeol. Anthropol. Sci. 2020;**12**:260. doi:10.1007/s12520-020-01128-9.
[47] Monatshebe T, Mulaba-Bafubiandi AF, Nyembwe DK. Mechanical properties and mineralogy of artisanal clay bricks manufactured in Dididi, Limpopo, South Africa. Constr. Build. Mater. 2019;**225**:972. doi:10.1016/j.conbuildmat.2019.07.247.
[48] Zouaoui H, Lecomte-Nana GL, Krichen M, Bouaziz J. Structure, microstructure and mechanical features of ceramic products of clay and non-plastic clay mixtures from Tunisia. Appl. Clay Sci. 2017;**135**:112. doi:10.1016/j.clay.2016.09.012.

(Rec. 10/03/2023, Rev. 16/10/2023, Rev. 01/12/2023, Ac. 12/12/2023)
(AE: A.E. Martinelli)